ADITUM
Enrich your Research

Case Reports International Journal

Research Article

Effect of Rare Ginsenosides of Li-Ginseng Powder on Cancer Cachexia Model Mice

Kwang-Il To[1], Myong-Hyon Ro[1], Chong-Hyok Han[2], Hyok-Chol Ri[1], Wen-Yuan Liu[3], Ying-Hua Jin[3], Su-Chol Rim[1*]

[1]Institute of Chemistry and Biology, University of Science, Pyongyang, DPR Korea.

[2]Clinical Faculty No 3., Pyongsong University of Medical Sciences, Pyongsong, DPR Korea.

[3]School of Life Sciences, Jilin University, Changchun, China.

Article Information

Received: May 28, 2026
Accepted: June 05, 2026
Published: June 12, 2026

***Corresponding author:** Su-Chol Rim, 3School of Life Sciences, Jilin University, Changchun, China.

Citation: Kwang-Il To, Myong-Hyon Ro, Chong-Hyok Han, Hyok-Chol Ri, Wen-Yuan Liu, Ying-Hua Jin, Su-Chol Rim., (2026). "Effect of Rare Ginsenosides of Li-Ginseng Powder on Cancer Cachexia Model Mice" Case Reports International Journal, 4(2); DOI: 10.61148/3065-6710/CRIJ/040.

Abstract

Cancer cachexia is a multifactorial syndrome characterized by rapid weight loss, skeletal muscle atrophy, and with or without fat reduction. Ginsenosides are important active components in ginseng. Previous studies have shown that some rare ginsenosides have anti-tumor and anti-inflammatory effects. In this study, we investigated the Li-ginseng powder on cachexia model mice by using various techniques such as enzyme-linked immunosorbent assay (ELISA), hematoxylin-eosin staining, protein western blotting, immunohistochemical staining, and immunofluorescence staining and network pharmacology. In animal experiments, compared with the normal group, mice in the cancer cachexia model group showed severe weight loss (approximately 16.5%, $P<0.0001$), while LGP significantly improved the body weight. The food intake of mice in the cachexia group decreased by approximately 3% compared with the normal group ($P<0.001$), but LGP significantly improved the appetite caused by cachexia. LGP significantly reduced the levels of TNF-α, IL-6, and IL-1β in serum ($P<0.0001$) and inhibited gastrocnemius muscle atrophy ($P<0.0001$). Through the experiment, We found that the phosphorylation levels of activated NF-κB and STAT3 were significantly upregulated in the cancer cachexia group but significantly inhibited by LGP, consistent with the expression levels of Trim63 and Fbxo32, indicating that the expression of Trim63 and Fbxo32 is regulated by the NF-κB and STAT3 signaling pathways. In addition, results showed that the expressions of Trim63, Fbxo32, p50 and STAT3 in C2C12 cells were significantly upregulated ($P<0.05$), while LGP significantly inhibited these protein expressions ($P<0.05$). In conclusion, LGP effectively inhibits weight loss and appetite decline in mice with cancer cachexia and significantly improves the reduction in gastrocnemius muscle, heart, and kidney weight. LGP significantly inhibits the activation of NF-κB and STAT3 in gastrocnemius muscle of mice with cancer cachexia, as well as the expression of E3 ubiquitin ligases Trim63 and Fbxo32, indicating that LGP effectively inhibits the occurrence of cancer cachexia.

Keyword: cancer cachexia, Ginsenoside, gastrocnemius, STAT3, NF-κB

Introduction

Cancer cachexia is a multifactorial syndrome that is closely related to poor prognosis. More than half of cancer patients show symptoms of cachexia, accounting for about 20% of all cancer-related deaths[1]. The development of cachexia is related to the type and stage of the tumor as well as the individual's physical condition. Currently, the standard for diagnosing

cachexia is still a weight loss of more than 5% or a body mass index (BMI) below 20[2, 3]. The main features of cachexia are systemic inflammation and weight loss, with reduced food intake being an important reason for weight loss. This can cause changes in energy balance, leading to lower energy intake than uptake. At the same time, the protein degradation and the decrease in muscle synthesis are also important reasons of weight loss, while the reduction of nutrients is a key factor leading to decreased protein synthesis. This highlights the importance of reduced dietary intake in cachexia[4, 5]. Although cancer cachexia has a huge impact on the quality of life and lifespan of patients, there is still no standardized nursing plan, which may be due to the unclear clinical definition. The lack of clinical data on nutritional support, other supportive care interventions, and new drug interventions, as well as the scarcity of preclinical data defining key mechanisms and targetable pathways, can all hinder research and treatment progress[6].

Currently, the main treatment method is to supplement nutrition to support the patient's consumption. In recent years, some peptide hormones, including Ghrelin and Anamorelin, have been developed to promote appetite and increase patient food intake, thereby allowing patients to obtain the necessary nutrients[7, 8]. Megestrol Acetate (MA) is a clinical drug for treating cachexia, but its main mechanism is to increase body fat rather than increase skeletal muscle mass[9]. Currently, the drugs used to treat cancer cachexia all have certain limitations, so current clinical treatments are beginning to look for reasonable multi-modal treatment plans. More researchers are also beginning to focus on drugs of cachexia, and in recent years, research on traditional Chinese medicine has provided a new direction for improving the current treatment of cachexia[10]. Traditional Chinese medicine represents a huge resource in modern medicine, and in recent years, understanding and application of Chinese herbs and preparations in evidence-based treatment has rapidly increased[11]. Preliminary laboratory research on the anti-tumor and anti-inflammatory effects of ginsenosides has been conducted[12-14], and further research is being conducted on the treatment of cancer cachexia. Li-Ginseng powder (LGP) from Yanbian ADKH Biotechnology Co., Ltd. is rich in a group of rare ginsenosides (GRGs) Rk1, Rk3, Rh4, Rg3, and Rg5. This study explored and verified the role of LGP in cancer cachexia through in vivo and in vitro experiments. Currently, the molecular mechanisms that cause muscle atrophy cannot be fully determined and are usually considered to be caused by an imbalance between protein synthesis and protein degradation. In cells, there are mainly two protein degradation metabolic pathways: the ubiquitin proteasome system (UPS) and the autophagic lysosome pathway (ALP), which are influenced by multiple circulating factors. Most misfolded proteins in cells are degraded by the UPS pathway, and skeletal muscle atrophy involves the E3 ubiquitin ligases Trim63 (also known as Murf1) and Fbxo32 (also known as atrogin-1) in the UPS pathway[15]. Fbxo32 is a muscle-specific protein highly expressed in atrophied muscle tissue, and it contains an F-Box conserved sequence that plays a functional role, classifying atrogin-1 as an FBXO protein in the F-box protein family, with X indicating its lack of a recognized substrate binding region. Trim63 is another muscle-specific protein that contains a TRIM tripartite motif and can regulate the degradation of myogenic differentiation protein (MyoD) and other proteins related to regulating muscle atrophy[16].

Tumor tissue can cause systemic inflammation and release a large number of inflammatory factors. Inflammatory factors lead to reduced tissue function, which is also a cause of cancer cachexia [17, 18]. TNF-α, IL-1β, and IL-6 are the main inflammatory factors persistently upregulated in cachexia[19]. The catabolic metabolism pathway of skeletal muscle is stimulated by various factors, including oxidative stress, inflammatory cytokines, and glucocorticoids, ultimately leading to the upregulation of E3 ubiquitin ligases Fbxo32 and Trim63[20]. Inflammatory factors are excessively released in cancer cachexia, activating multiple signaling pathways, including the NF-κB and STAT3 pathways. Inflammatory cytokines such as tumor necrosis factor a (TNF-a), interleukin-6 (IL-6), and interleukin-1β (IL-1β) can cause muscle atrophy by regulating the NF-κB and STAT3 pathways[21, 22].

In recent years, a large number of studies have proved that the above pathways can generate cachexia, leading to skeletal muscle atrophy and preventing muscle regeneration[23-25]. When cells are affected by extracellular signals (such as TNF-α, IL-1β, or IL-6), NF-κB is activated, regulating the UPS pathway, leading to the upregulation of Trim63 and Fbxo32 expression, and targeting MyoD, thereby affecting muscle differentiation [26, 27]. The NF-κB inhibitor SN50 can reduce the expression of proteasome 20S subunits, thereby inhibiting muscle atrophy [28]. The STAT3 signaling pathway plays a role in various cellular activities, including cell growth, proliferation, differentiation, and apoptosis [29]. Related studies have shown that STAT3 expression is upregulated in cancer cachexia, p-STAT3 expression is upregulated in mouse skeletal muscle, and the STAT3 signaling pathway can activate the expression of C/EBPδ, stimulate the activation of downstream MAFbx and MuRF1, and cause muscle atrophy[30].

Materials and methods

Reagents

Li-Ginseng powder (LGP) enriched with rare ginsenosides including Rk1, Rk3, Rh4, Rg3, and Rg5 was provided by Yanbian ADKH Biotechnology Co., Ltd. Imperatorin (IMP) was purchased from Shanghai EFEBIO Biological Co., Ltd. DMEM high glucose medium, 1640 medium, and fetal bovine serum were purchased from Gibco (New York, USA), while horse serum was purchased from KangYuan Biological Co., Ltd. Fbxo32 antibody, Trim63 antibody, and MyoD antibody were purchased from Proteintech, while STAT3 antibody, p-STAT3 antibody, p50 antibody, p-p50 antibody, p65 antibody, and p-p65 antibody were purchased from Santa Cruz. GAPDH antibody was purchased from Cell Signaling Technology, Pierce Goat Anti-Mouse IgG and Pierce Goat Anti-Rabbit IgG were purchased from Thermo Scientific.

Cell culture

CT26 mouse colon cancer cells were obtained from Shanghai Enzyme Research Science and Technology Bioengineering Co., Ltd., and were cultured in RPMI 1640 medium containing 10% (v/v) fetal bovine serum, 100 U/mL penicillin, and 100 μg/mL streptomycin under conditions of 5% CO2, 37°C, and saturation humidity. C2C12 mouse myoblasts were obtained from Shanghai EK-BIOscience Co., Ltd. and were cultured in DMEM medium containing 10% (v/v) fetal bovine serum, 100 U/mL penicillin, and 100 μg/mL streptomycin under conditions of 5% CO2, 37°C, and saturation humidity. The differentiation of C2C12 cells was induced by replacing the growth medium with DMEM medium containing 2% horse serum once the cells were in the logarithmic growth phase. The medium was changed every day until the cells

differentiated into multinucleated myotubes, which could be used for subsequent experiments.

Animals

Six-week-old male Balb/c mice with a bodyweight of 20±2 g were purchased from Beijing vitalriver Technology Co., Ltd. (SCXK (Jing) 2021-2006).

In vitro experiments

C2C12 cells were seeded in a 96-well plate and cultured in DMEM medium containing 2% horse serum until they reached the logarithmic growth phase. When the cells differentiated into multi-nuclear muscle tubules, the medium containing different concentrations of LGE was changed, and the concentrations of LGE were set as 0, 1, 2.5, 5, 7.5, 10, 20, 50 mg/mL. And then, the absorbance at 570 nm was measured with a microplate reader.

Collection of tumor-conditioned medium

Tumor-conditioned medium (TCM) was prepared by culturing CT26 cells in DMEM medium containing 2% horse serum until they reached the logarithmic growth phase. After 48 hours of culture, the medium was collected and centrifuged at 1000 rpm for 10 minutes to obtain the supernatant for use in the establishment of an in vitro cachexia model.

In vitro cancer cachexia model:

To establish an in vitro model, when C2C12 cells differentiated into myotubes, the original culture medium was discarded and tumor-conditioned medium was mixed with normal culture medium at a ratio of 1:1. The mixture was added to the culture dish to induce atrophy of the myotubes. LGP treatment was added for 48 hours, and then the cells were collected for subsequent testing. For the control group, C2C12 cell supernatants were mixed with normal culture medium at a ratio of 1:1.

In vivo cancer cachexia model:

The study selected CT26 colon cancer cells and SPF male Balb/c mice to construct a cancer cachexia model. This model has been widely accepted and used in the study of the pathogenesis of cancer cachexia and screening of candidate drugs. CT26 colon cancer cells were made into 100 μL (1.0×10^6 cells/mL) and injected subcutaneously into the right axillary fossa of mice. After approximately 7 days, obvious tumor masses could be observed, and after 14 days, the mice were euthanized, and the tumor masses were harvested, crushed with scissors, filtered through a 200-mesh sieve, and made into a tumor tissue suspension. The second-generation mice were injected subcutaneously with 100 μL of the tumor tissue suspension in the right axillary fossa to form typical cachexia more easily.

The study was divided into five groups: Control (healthy mice), Model (injection of 100 μL of tumor tissue suspension, cancer cachexia model group), LGP low-dose group (LGP(L), injection of 100 μL of tumor tissue suspension, after visible tumors appeared, LGP was administered orally gavage of 85 mg/kg), LGP high-dose group (LGP(H), LGP was administered orally gavage of 170 mg/kg), and positive control group (IMP, injection of 100 μL of tumor tissue suspension, after visible tumors appeared, IMP was administered orally gavage of 50 mg/kg). After the second-generation mice were implanted with tumors, daily food intake and weight were measured. On the 18th day, the mice were euthanized and their blood, heart, liver, spleen, lungs, kidneys, and gastrocnemius muscles were collected for further testing.

Histological examination staining:

The mouse gastrocnemius muscle was fixed in 4% paraformaldehyde solution and embedded in paraffin. The tissue was then cut into 4-μm sections, placed on slides, and baked at 60°C for 30 minutes. The paraffin sections were then subjected to dewaxing, rehydration, hematoxylin staining, differentiation, eosin staining, dehydration, transparency, sealing, and microscopic analysis.

Immunohistochemistry staining:

The mouse gastrocnemius muscle sections were subjected to dewaxing and antigen retrieval, followed by blocking with non-specific staining blocker at room temperature for 20 minutes. The primary antibody was diluted with antibody diluent and added to the sections, which were then placed in a wet box and incubated at 4°C for at least 12 hours. Biotin-labeled goat anti-mouse/rabbit IgG polymer was added to the sections, followed by incubation for 20 minutes. Streptavidin-biotin-peroxidase was added and incubated for 20 minutes. Diaminobenzidine (DAB) chromogenic solution was added to the sections, which were then terminated with PBS and restained with hematoxylin. After dehydration and transparency, neutral resin was used to seal the sections, which were then analyzed by microscopy.

Western blot:

Protein sample preparation:

C2C12 cells were transferred to a 1.5 mL centrifuge tube. RIPA lysis buffer (with 1% PMSF and phosphatase inhibitor added) was added and incubated on ice for 50 minutes. The lysed cells were centrifuged at 12000 rpm for 15 minutes at 4°C. The supernatant was absorbed and BCA protein was quantified. The sample was boiled with 5×Loading Buffer and inactivated in boiling water for 5 minutes. Protein samples were stored at -20°C for subsequent use.

Mouse gastrocnemius muscle was ground in the grinding instrument; and incubated on ice for 50 minutes. The lysate was centrifuged at 12000 rpm for 15 minutes at 4°C, and the supernatant was collected. BCA protein quantification was performed, and the sample was boiled with 5×Loading Buffer and stored at -20°C for subsequent use.

Polyacrylamide gel electrophoresis (SDS-PAGE):SDS-PAGE gel was prepared, and equal amounts of protein samples were separated on the gel. The separated proteins were transferred onto polyvinylidene fluoride (PVDF) membranes, which were blocked with 5% skimmed milk powder for 1 hour. The primary antibody was diluted in 3% skimmed milk powder and incubated overnight at 4°C. The secondary antibody was diluted in 3% skimmed milk powder and incubated for 1 hour. ECL Chemiluminescent Kit (Thermo Fisher, Waltham, MA, United States) was used to visualize the antibody–antigen interaction, and chemical luminescence of membranes was detected by Tanon 5200.

Measurement of inflammatory cytokines in serum:

Enzyme-linked immunosorbent assay kits (mouse TNF-α, mouse IL-6, and mouse IL-1β assay kits; Jianglai Biotechnology Co., Ltd., China) were used.

Detected of rare ginsenoside content in LGP:

Alcohol extraction was used to extract the substances contained in LGP, and purified analysis of the extracted substances was performed using high-performance liquid chromatography (HPLC). The mobile phase of HPLC was 20% acetonitrile plus 80% methanol. LGP extract was dissolved in methanol, and the standard sample was a mixture containing Rg5, Rg1, Rg3, Rb1, Rb2, Rk1, Rh4, Re, Rd, Rc, Rf, F1, and F2.

Network topology analysis:

BATMAN-TCM (http://bionet.ncpsb.org.cn/batman-tcm) and PubChem (https://pubchem.ncbi.nlm.nih.gov) were used to screen for the targets of Rk1, Rk3, Rh4, Rg3, and Rg5, and the obtained targets from both databases were merged to obtain all targets. Cytoscape software was used to construct a drug-target network.

DisgeNET (https://www.disgenet.org/), GeneCard (https://www.genecard.org/), and OMIM (https://www.omim.org/) databases were searched with "cancer cachexia" as the keyword to select disease targets related to cancer cachexia. The obtained targets from the three databases were sorted and merged to obtain all disease targets.

The Venny2.1.0 website

(https://bioinfogp.cnb.csic.es/tools/venny/) was used to sort the targets of Rk1, Rk3, Rh4, Rg3, and Rg5 and cancer cachexia disease targets, and the intersection of the two was taken as the potential targets of the rare ginsenosides in cancer cachexia. Using the STRING database (https://cn.string-db.org/), an interaction network was generated, and a "ginsenoside-cancer cachexia" PPI interaction network was constructed using Cytoscape based on the downloaded tsv file, analyzing the correlation of each target according to Degree.

Gene ontology and pathway enrichment analysis:

Metascape (https://metascape.org/gp/index.html) was used to perform GO and KEGG pathway enrichment analysis on the targets of rare ginsenosides in cancer cachexia, to explore the biological processes and signaling pathways through which ginsenosides play a role in cancer cachexia.

Experimental data analysis:

GraphPad Prism 8 software was used for experimental data analysis and processing. One-way ANOVA was used for statistical analysis, and a P-value of <0.05 was considered statistically significant.

Result

3.1 LGP significantly improved the body weight and food intake of C26 tumour-bearing mice

Cancer cachexia leads to rapid weight loss and systemic inflammation in patients, and there is currently no effective treatment. Previous studies by the research team found that Li-Ginseng powder (LGP) significantly inhibited inflammation and tumor occurrence in a mouse model of inflammatory colon cancer. LGP is characterized by its high-activity of rare ginsenosides (Rg3, Rg5, Rk1, Rk3, Rh4). This study investigated the inhibitory effect of LGP on cancer cachexia in a Balb/c mouse model. The study used a tumor suspension from the subcutaneous tumors of first-generation mice to induce tumors in the right axillary subcutaneous tissue of second-generation mice to establish the cancer cachexia model (Figure 1A). Treatment began on the third day when the tumor mass was palpable. The tumor weight was calculated using the formula: tumor weight (g) = 0.52 × tumor length (cm) × tumor width^2 (cm)[31]. On the seventh day, compared with the control group, the body weight of the Model group began to decrease significantly (by about 6.7%); on the seventeenth day, the body weight of the Model group decreased by about 16.5%. After treatment with LGP and IMP, the body weight of the LGP (H) group was basically the same as that of the control group; the body weight of the LGP (L) group decreased by about 4%; and the body weight of the IMP group decreased by about 3% (Figure 1B). Loss of appetite is also a reason for rapid weight loss, so the food intake of each group was monitored. The results showed that the food intake of the control and treatment groups remained stable, while the food intake of the model group decreased significantly (Figure 1C).

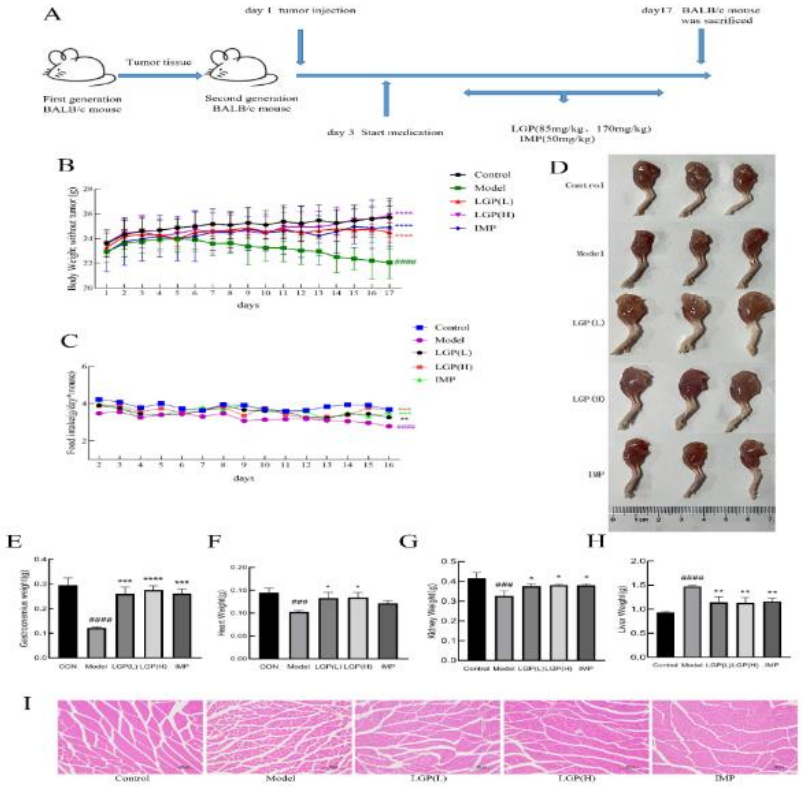

Figure 1 LGP can significantly improve cancer cachexia. (A) Establishment of CT26 mouse colon cancer cachexia model; (B) Body weight change curve of mice in each group; (C) Food intake change curve of mice in each group; (D) Photographs of mouse leg muscles; (E) Gastrocnemius muscle weight of mice in each group; (F) Heart weight of mice in each group; (G) Kidney weight of mice in each group; (H) Liver weight of mice in each group; (I) HE staining of mouse gastrocnemius muscle (100×); # indicates compared to the Control group, * indicates compared to the model group, $^{\#}P<0.05$, $^{\#\#}P<0.01$, $^{\#\#\#}P<0.001$, $^{\#\#\#\#}P<0.0001$, $^{*}P<0.05$, $^{**}P<0.01$, $^{***}P<0.001$, $^{****}P<0.0001$.

3.2 LGP inhibited the gastrocnemius atrophy and affected the weight of organ

As shown in Figure 1D, the leg muscles of cancer cachexia mice were significantly atrophied, while the atrophy of leg muscles in the LGP and IMP groups of mice was significantly reduced. Cancer cachexia may have bad effects on various tissues and organs of the body. To investigate the effects of LGP on the various tissues and organs of cancer cachexia mice, the gastrocnemius muscle, heart, liver, spleen, kidney, and lung of each group of mice were weighed and compared. The results showed that compared with control, the organs and gastrocnemius muscle of model group produced significant changes in weight ($P<0.05$).

The weight of the gastrocnemius muscle (Figure 1E), heart (Figure 1F), and kidney (Figure 1G) in the model group decreased significantly ($P<0.05$), and was effectively improved after LGP treatment ($P<0.05$). The improvement in the gastrocnemius muscle was particularly significant ($P<0.0001$). The liver (Figure 1H) weights increased significantly in the model group ($P<0.05$), but after LGP treatment, the liver weight decreased significantly compared with the cancer cachexia group. This indicates that cancer cachexia leads to changes in the weight of various organs and the gastrocnemius muscle in mice, and LGP treatment significantly improves these changes.

The typical characteristic of cancer cachexia is the degradation of muscle tissue leading to a decrease in muscle mass. The changes in muscle fibers were observed by HE staining of paraffin sections of the gastrocnemius muscle in mice (Figure 1I). The results showed that compared to the control group, the model group had muscle fiber atrophy and increased gaps between muscle fibers. LGP and IMP treatment significantly improved muscle fiber atrophy in cancer cachexia mice, indicating that LGP effectively improved the degradation of skeletal muscle fibers in cancer cachexia.

3.3 LGP ameliorated myofibre and inhibits muscle atrophy by down-regulating the expression of Fbxo32 and Trim63

The degradation of skeletal muscle is mainly carried out through the UPS and autophagy. In the process of cancer cachexia, the UPS pathway is the main pathway of the degradation of skeletal muscle. The expression of two E3 ligases, Fbxo32 and Trim63 was increases, resulting in skeletal muscle atrophy. Immunohistochemical staining was performed to detect the expression of Fbxo32 and Trim63 proteins. As shown in Figure 3E, compared to control group, the expression levels of Fbxo32 and Trim63 in the gastrocnemius muscle of the model group were significantly upregulated, while the expression levels of Fbxo32 and Trim63 in the LGP and IMP treatment groups were significantly decreased compared to the model group. Western blot was used to detect the expression levels of Fbxo32 and Trim63 in the gastrocnemius muscle of each group (Figure 2F). Compared to the control group, the expression levels of Fbxo32 and Trim63 in the gastrocnemius muscle of the model group were significantly upregulated, indicating that the degradation of skeletal muscle increased in the model group. The expression levels of Fbxo32 and Trim63 were significantly decreased in the LGP and IMP treatment groups (Figures 2F, G, and H). The expression levels of the MyoD were detected (Figures 2F and I), and the results showed that the expression of MyoD was inhibited in the gastrocnemius muscle of the model group, while the expression of MyoD was significantly upregulated in the LGP group after treatment.

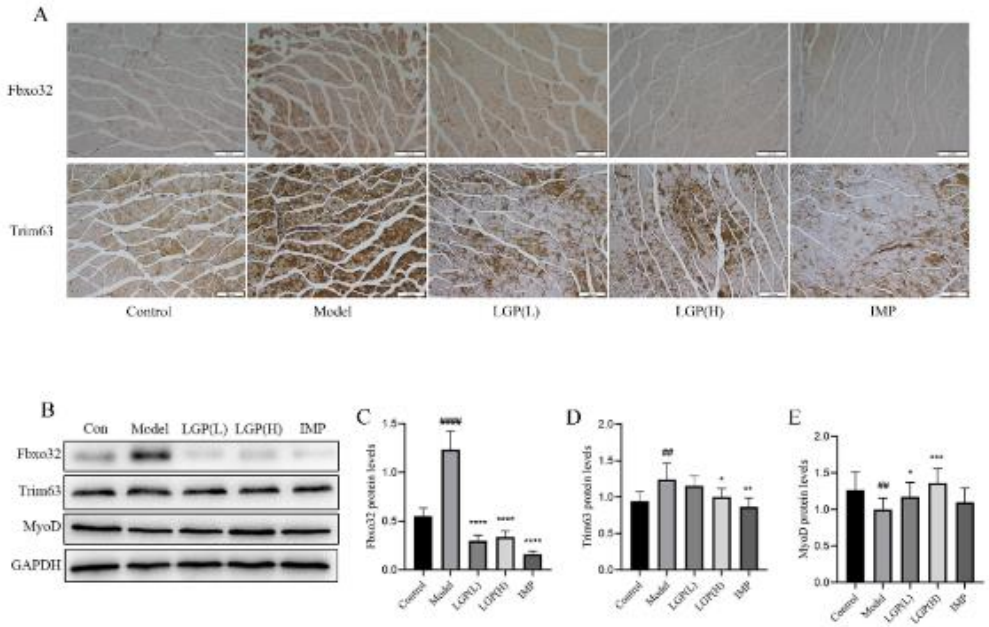

Figure 2: LGP inhibits muscle atrophy by regulating the UPS pathway. (A) Immunohistochemical staining of Fbxo32 and Trim63 expression in mouse gastrocnemius muscle (100×); (B) Western blot analysis of Fbxo32, Trim63, and MyoD expression in mouse gastrocnemius muscle; (C) Expression level of Fbxo32; (D) Expression level of Trim63; (E) Expression level of MyoD. # indicates compared to the Control group, * indicates compared to the model group, $^{\#}P<0.05$, $^{\#\#}P<0.01$, $^{\#\#\#}P<0.001$, $^{\#\#\#\#}P<0.0001$, $^{*}P<0.05$, $^{**}P<0.01$, $^{***}P<0.001$, $^{****}P<0.0001$.

3.4 The content of ginsenoside in LGP ethanol extract accounts for about 60%, which has 121 potential targets for cancer cachexia

The active in Li-Ginseng extract (LGE) were extracted from LGP using ethanol extraction, and the content of ginsenosides Rk1, Rk3, Rh4, Rg3, and Rg5 in LGE was identified by high-performance liquid chromatography (HPLC). The results showed that the contents of ginsenosides Rk1, Rk3, Rh4, Rg3, and Rg5 in LGE were 12.94%, 5.67%, 11.31%, 10.68%, and 17.97%, respectively, accounting for about 60% of the total extract (Figure 3A).

The rare ginsenosides Rk1, Rk3, Rh4, Rg3, and Rg5 contained in LGP were searched for 57, 46, 42, 98, and 88 target proteins, respectively, and after removing duplicates, 199 ginsenoside target proteins were obtained (Figure 3B). A total of 2891 disease target proteins were obtained by searching for cancer cachexia in DisgeNET (110 targets), GeneCard (2562 targets), and OMIM (496 targets) (Figure 3C). The potential target proteins of the rare ginsenosides in cancer cachexia were obtained by integrating the target proteins of the rare ginsenosides and the disease target proteins of cancer cachexia using the Venny2.1 tool, and a total of 121 potential target proteins were obtained (Figure 3D).

The 121 target proteins were used to construct a PPI network using the STRING database, which contained 121 nodes and 2581 edges. Network analysis was performed using Cytoscape software, and AKT1, TP53, CASP3, and STAT3 were found to occupy a central position in the network, while NF-κB was found to be important (Figure 3E).

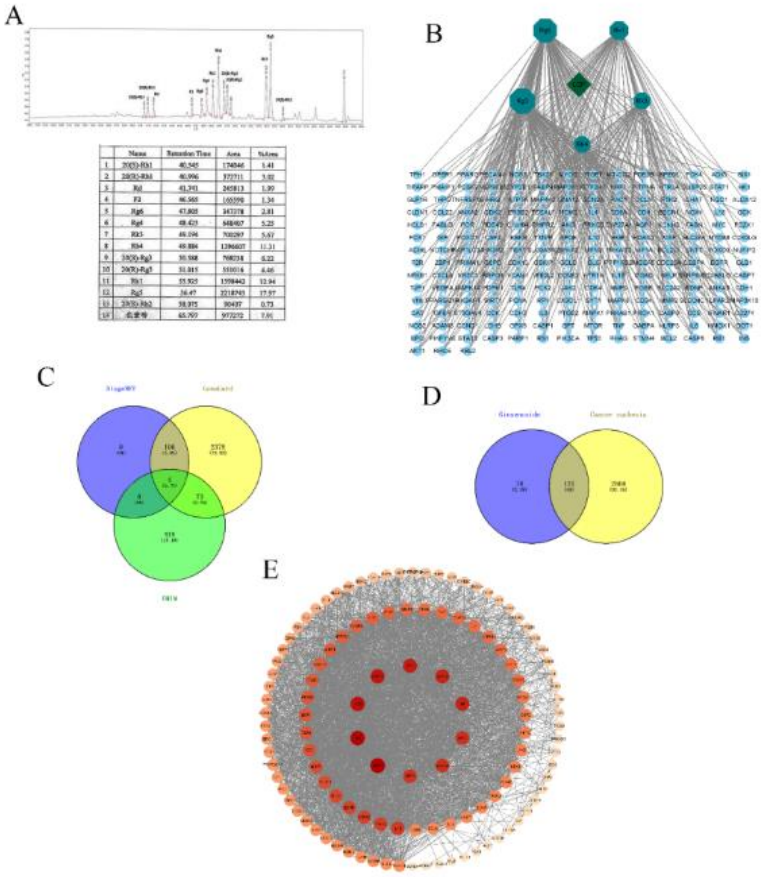

Figure 3: Rare ginsenosides and targets for cancer cachexia. (A) The content of ginsenosides in LGP ethanol extract; (B) Diagram of 199 rare ginsenoside target points; (C) 2981 targets for cancer cachexia; (D) Venn diagram of targets for cancer cachexia and rare ginsenoside target points; (E) PPI interaction network between rare ginsenosides and cachexia in cancer.

3.5 Ginsenosides inhibit cancer cachexia by regulating STAT3 and NF-κB pathways

The 121 common target proteins were analyzed using Metascape for GO analysis and KEGG enrichment analysis. The results of the GO analysis showed that the 121 common target proteins were mainly involved in kinase binding, protein kinase activity, transcription factor binding, and cytokine receptor binding in terms of molecular function (MF) (Figure 4A); response to hormone, response to inorganic substance, positive regulation of phosphorylation, response to lipopolysaccharide, regulation of neuron death, positive regulation of cell death and positive regulation of cell motility in biological process (BP) (Figure 4B); and membrane raft, side of membrane, transcription regulator complex, transferase complex, and receptor complex in cellular component (CC) (Figure 4C). The KEGG pathway enrichment analysis revealed that the common targets of rare ginsenosides and

cancer cachexia were mainly involved in cancer pathways, lipid and atherosclerosis, FoxO signaling pathway, proteoglycans in cancer, MAPK signaling pathway, and NF-κB signaling pathway (Figure 4D).

LGP reduces the levels of inflammatory cytokines TNF-α, IL-6, and IL-1β in serum. Cancer cachexia can cause systemic inflammation, leading to an increase in the levels of related inflammatory factors in serum. To investigate the effect of LGP on inflammation in cancer cachexia, the levels of TNF-α, IL-6, and IL-1β in mouse serum were measured. The results showed that compared with the normal group of mice, the levels of TNF-α, IL-6, and IL-1β in the serum of the model group increased significantly (P<0.0001), and after LGP and IMP treatment, the levels of TNF-α, IL-6, and IL-1β in the serum of the mice decreased significantly (P<0.0001) (Figure 4E, F, and G). This indicates that LGP can reduce the levels of TNF-α, IL-6, and IL-1β in mouse serum, thereby inhibiting systemic inflammation.

The NF-κB and STAT3 signaling pathways regulated the expression of the ubiquitin ligases Fbxo32 and Trim63 in the ubiquitin-proteasome system. The expression and activation status of the NF-κB subunits p50 and p65 and STAT3 in the gastrocnemius muscle, as well as the degree of phosphorylation at key sites, p-p65 (Ser536), p-p50 (Ser337), and p-STAT3 (Tyr705), were analyzed. The results showed that the NF-κB (Figure 4H, I, and J), p65 (Figure 4H, K, and L), and STAT3 (Figure 4H, M, and N) signaling pathways were activated in the model group compared to the control, and the activation of these pathways was inhibited by LGP and IMP treatment. This suggests that LGP inhibits the degradation of muscle in cancer cachexia mice by suppressing the activation of the NF-κB and STAT3 signaling pathways.

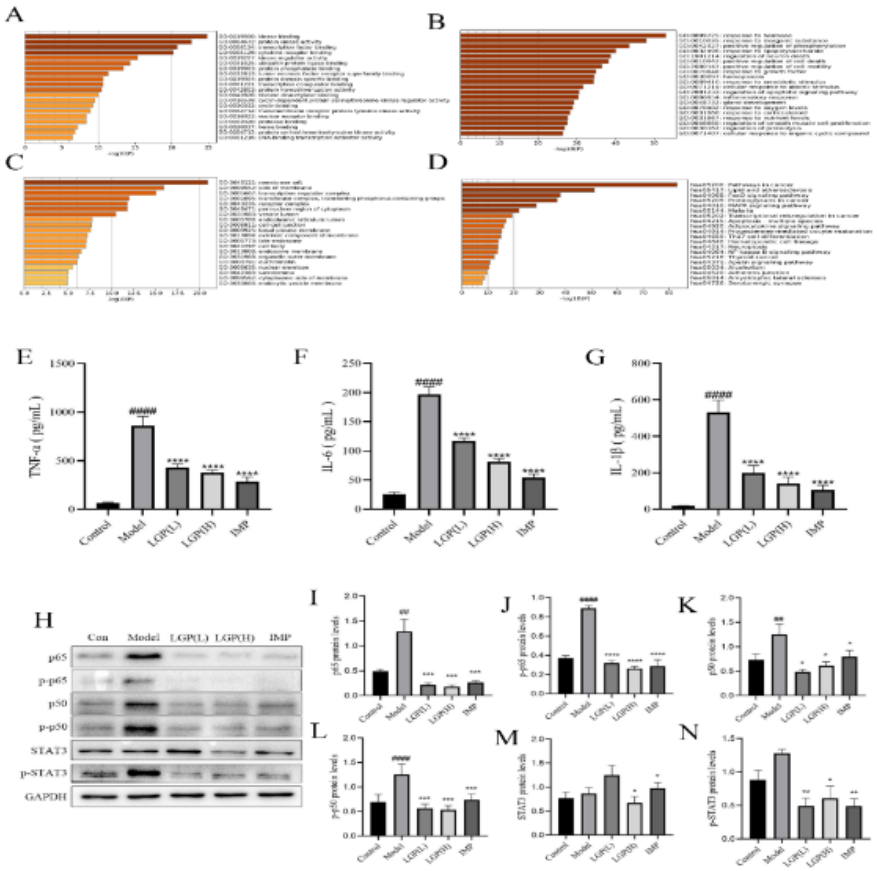

Figure 4: PPI network, GO and KEGG enrichment analysis of rare ginsenosides and cachexia in cancer. (A) Molecular function analysis of GO; (B) Biological process analysis of GO; (C) Cellular component analysis of GO; (D) KEGG enrichment analysis; (E) The content of TNF-α in the serum of each group of mice; (F) The content of IL-6 in the serum of each group of mice; (G) The content of IL-1β in the serum of each group of mice; (H) Regulation of signaling pathways related to cachexia in cancer by LGP; (I) Expression level of p65; (J) Expression level of p-p65; (K) Expression level of p50; (L) Expression level of p-p50; (M) Expression level of STAT3; (N) Expression level of p-STAT3. # indicates compared to the Control group, * indicates compared to the model group, $^{\#}P$<0.05, $^{\#\#}P$<0.01, $^{\#\#\#}P$<0.001, $^{\#\#\#\#}P$<0.0001, $^{*}P$<0.05, $^{**}P$<0.01, $^{***}P$<0.001, $^{****}P$<0.0001.

3.6 LGE alleviated myotube atrophy in an in vitro model of cancer cachexia and affected NF-κB and STAT3 signaling pathways in C2C12 myotubes

Differentiation of C2C12 mouse myoblasts showed that cell fusion occurred on the fifth day, forming myotubes (Figure 5A). To determine whether LGE affects the viability of myotube cells, the activity of C2C12 myotubes was measured using the MTT assay at different concentrations of LGE. The experimental results showed that LGE had no toxic effect on C2C12 myotubes at concentrations below 20 μg/mL (Figure 5C).

To verify whether LGE has a protective effect on myotubes induced under conditions of cancer cachexia, C2C12 cells were

induced with TCM and treated with 15 μg/mL and 20 μg/mL LGE, respectively. IMP was used as a positive control, and the cells were treated for 48 hours. HE staining showed that the myotubes induced by TCM became sparse and had a shorter diameter, indicating that the myotubes had atrophied. Treatment with LGE and IMP significantly improved the atrophy of myotubes (Figure 5B).

Immunofluorescence staining showed that compared with the normal group, the expression of Fbxo32 and Trim63 was upregulated in the myotubes induced by TCM. After treatment with LGE and IMP, the expression of Fbxo32 and Trim63 was downregulated compared with that in the TCM-treated group (Figure 5D). Western blot analysis was used to detect the expression of Fbxo32 and Trim63 in myotubes. The results showed that the expression levels of Fbxo32 and Trim63 were significantly upregulated in the myotubes treated with TCM (P<0.05). After treatment with LGE, the expression levels of Fbxo32 and Trim63 were significantly downregulated compared with those in the TCM-treated group (P<0.05) (Figures 5C, F, and G). The expression of MyoD was also detected, and it was found that the expression level of MyoD was significantly upregulated compared with that in the TCM-treated group (P<0.05) (Figures 5C and H).

Related studies have shown that in cancer cachexia, the NF-κB and STAT3 signaling pathways are activated, leading to upregulation of Fbxo32 and Trim63 expression. Therefore, the expression of the NF-κB subunit p50 and STAT3 was detected. The results showed that under TCM treatment conditions, the phosphorylation levels of p50 and STAT3 were significantly upregulated compared with those in the control group. After treatment with LGE, the phosphorylation levels of p50 and STAT3 were significantly downregulated (P<0.05) (Figures 5A, C, and E). This indicates that Fbxo32 and Trim63 can improve myotube atrophy caused by cancer cachexia by inhibiting the NF-κB and STAT3 signaling pathways.

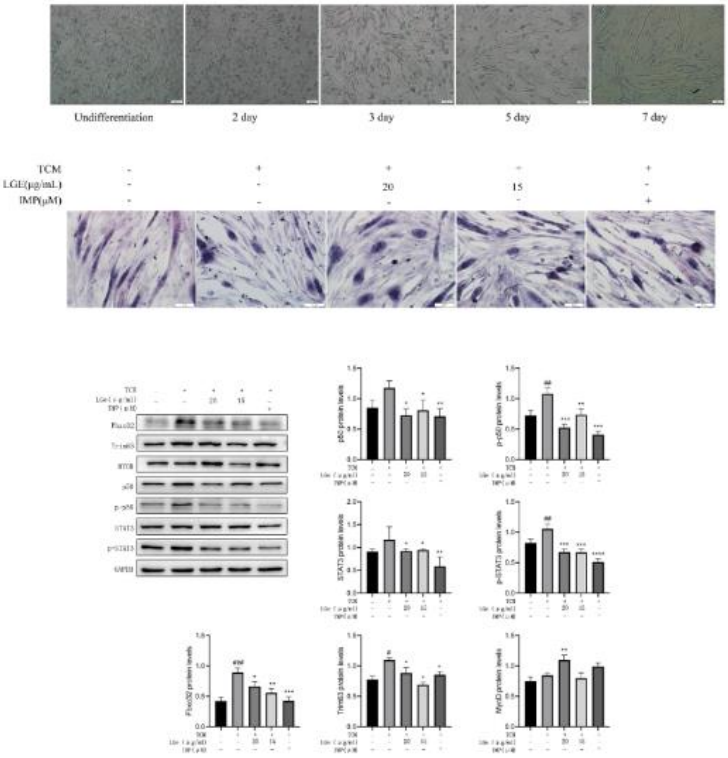

Figure 5: LGE inhibits the atrophy of C2C12 cells (A) Horse serum induced C2C12 cells to differentiate into muscle tubes; (B) HE staining of muscle tubes; (C); (D); (E); (F) Regulation of signaling pathways related to cachexia in cancer by LGP; (G) Expression level of p65; (H) Expression level of p-p65; (I) Expression level of p50; (J) Expression level of p-p50; (K) Expression level of STAT3; (L) Expression level of p-STAT3. # indicates compared to the Control group, * indicates compared to the model group, $^{\#}P$<0.05, $^{\#\#}P$<0.01, $^{\#\#\#}P$<0.001, $^{\#\#\#\#}P$<0.0001, $^{*}P$<0.05, $^{**}P$<0.01, $^{***}P$<0.001, $^{****}P$<0.0001.

Discussion

Cancer cachexia is a multifactorial syndrome characterized by rapid loss of muscle mass. More than half of cancer patients suffer from cachexia, which has a significantly adverse impact on their lives and survival[2, 3]. Cachexia can cause rapid degradation of muscle tissue and fat tissue, resulting in serious damage to organs in the body. The specific pathogenesis of cachexia is currently unclear, but studies have shown that tumor secretions, tumor-induced immune reactions, and metabolic changes are closely related to its pathogenesis [32]. In recent years, ginseng has been used as an important traditional Chinese medicine containing rare ginsenosides, including Rk1, Rk3, Rh4, Rg3, and Rg5, which have been used to treat various diseases, including cancer, hypertension, and inflammation. This study focuses on the effect of LGP, which contains these rare ginsenosides, on the gastrocnemius muscle and related signaling pathways in cancer cachexia.

A CT26 colon cancer cachexia mouse model was established for this study, which has been widely used in the research of cancer cachexia. The first-generation mice were transplanted with tumor

cells, and the second-generation mice were transplanted with the cells in the right upper limb axilla. The results showed that the second-generation mice exhibited more typical characteristics of cancer cachexia than the first-generation tumor-bearing mice, showing more significant weight loss, reduced food intake, and accompanied by a significant decrease in heart and kidney weight. After successful modeling, LGP was used to treat cancer cachexia mice, and it was found that LGP significantly alleviated the rapid weight loss in cachexia mice and had a positive impact on their food intake. The levels of TNF-α, IL-6, and IL-1β in the serum of each group of mice were detected, and it was found that compared with the normal group of mice, the levels of TNF-α, IL-6, and IL-1β in the serum of cancer cachexia group of mice were significantly increased. After LGP treatment, the levels of TNF-α, IL-6, and IL-1β in the serum of mice were significantly decreased, indicating that LGP has an excellent inhibitory effect on systemic inflammation. Analysis of the gastrocnemius muscle of mice showed that LGP significantly inhibited atrophy and mass loss, protecting the activity of the gastrocnemius muscle in mice. Further analysis using HE staining and protein immunoblotting showed that the STAT3 signaling pathway and NF-κB signaling pathway were activated in the cachexia group of mice, and the expression levels of Fbxo32 and Trim63 were significantly upregulated. After LGP treatment, the activation of the STAT3 signaling pathway and NF-κB signaling pathway was effectively inhibited, and the expression levels of Fbxo32 and Trim63 were significantly downregulated.

LGP has a significantly therapeutic effect on cancer cachexia. To study its mechanism of action, network pharmacology was used to analyze the rare ginsenosides contained in LGP and the disease targets related to cancer cachexia. Network pharmacology is an emerging discipline based on systems biology theory, which emphasizes the importance of developing rational and effective drugs through the multiple regulation of signaling pathways. In this study, the interaction network was constructed using PPI to screen core proteins, and AKT1, TP53, CASP3, INS, STAT3, and NF-κB were identified as potential core proteins for the inhibitory effect of ginsenosides on cancer cachexia. The STAT3 signaling pathway and NF-κB signaling pathway play a key role in the pathogenesis of cancer cachexia, and LGP's main rare ginsenosides, Rg5, Rk1, and Rh4, can inhibit the STAT3 signaling pathway and NF-κB signaling pathway. Therefore, this study analyzed the activation status of STAT3 and NF-κB in gastrocnemius muscle tissue. It is exciting to find that both transcription factors were activated in the cachexia model, while LGP treatment significantly inhibited their activation. Meanwhile, the expression of muscle fiber-specific E3 ligases Fbxo32 and Trim63 was significantly upregulated in the model group, and LGP treatment significantly inhibited the expression of these proteins.

We further explored the effect of LGP's ethanol extract LGE on cancer cachexia cell models through in vitro cell experiments. Western Blot analysis showed that LGE treatment effectively inhibited the activation of the STAT3 and NF-κB signaling pathways in cachexia myotube cells, thereby inhibiting the expression of muscle-specific E3 ubiquitin ligases Fbxo32 and Trim63 and blocking the degradation of MyoD. The results indicate that LGE improves the progression of cancer cachexia by inhibiting the ubiquitination and degradation pathway of myotube cells.

Both animal models and in vitro cell models have shown that LGP significantly inhibits muscle atrophy during cancer cachexia. This study only investigated the mechanism by which LGP inhibits muscle atrophy and did not explore its mechanisms for improving heart and kidney function, which should be addressed in future studies.

As a common syndrome in late-stage cancer patients, cancer cachexia is influenced by multiple factors that seriously affect the quality of life and survival rate of cancer patients. More and more reaserch result show that targeting a single molecule or pathway is insufficient to effectively treat multifactorial and multisystem cancer cachexia. Multi-modal treatment methods, including drug, nutrition, and exercise intervention, have received widespread attention and may be beneficial for treating this disease. LGP contains a variety of rare ginsenosides, ginseng polysaccharides, and ginseng peptides. In this study, we found that LGP treatment can simultaneously regulate multiple signaling pathways involved in cancer cachexia, including the NF-κB and STAT3 signaling pathways, while effectively inhibiting systemic inflammation. This may explain the good therapeutic effect of LGP. Combining LGP treatment with nutrition and exercise interventions may achieve better therapeutic outcomes, and this possibility needs to be further explored.

Conclusion

LGP effectively inhibits weight loss and appetite decline in mice with cancer cachexia and significantly improves the reduction in gastrocnemius muscle, heart, and kidney weight. LGP significantly inhibits the activation of NF-κB and STAT3 in gastrocnemius muscle of mice with cancer cachexia, as well as the expression of E3 ubiquitin ligases Trim63 and Fbxo32, indicating that LGP effectively inhibits the occurrence of cancer cachexia. Therefore, we believe that Li-Ginseng powder has promising potential as an effective drug for the treatment of cancer cachexia.

Acknowledgement

We thank the participants who were all contributed samples to the study. Especially, the authors would like to express their gratitude to professor Ying-Hua Jin for her correct guidance and valuable recommendation.

Funding

This study has not received any external funding.

Conflict of Interest

The authors declare that there are no conflicts of interests.

Ethical approval

All animal experiments were conducted according to the regulations of the Administration of Affairs Concerning Experimental Animals in China. The protocol was approved by the Institutional Animal care and Use Committee of Jilin University (20170318).

Informed consent

Not applicable.

Data materials availability

All data associated with this study are present in the paper.

References:

1. SIDDIQUI J A, POTHURAJU R, JAIN M, et al. Advances in cancer cachexia: Intersection between affected organs, mediators, and pharmacological interventions [J]. Biochim Biophys Acta Rev Cancer, 2020, 1873(2): 188359.

2. BARACOS V E, MARTIN L, KORC M, et al. Cancer-associated cachexia [J]. Nat Rev Dis Primers, 2018, 4: 17105.
3. FEARON K, STRASSER F, ANKER S D, et al. Definition and classification of cancer cachexia: an international consensus [J]. Lancet Oncol, 2011, 12(5): 489-95.
4. FRIESEN D E, BARACOS V E, TUSZYNSKI J A. Modeling the energetic cost of cancer as a result of altered energy metabolism: implications for cachexia [J]. Theor Biol Med Model, 2015, 12: 17.
5. HALL K D, BARACOS V E. Computational modeling of cancer cachexia [J]. Curr Opin Clin Nutr Metab Care, 2008, 11(3): 214-21.
6. GAAFER O U, ZIMMERS T A. Nutrition challenges of cancer cachexia [J]. JPEN J Parenter Enteral Nutr, 2021, 45(S2): 16-25.
7. NISHIE K, SATO S, HANAOKA M. Anamorelin for cancer cachexia [J]. Drugs Today (Barc), 2022, 58(3): 97-104.
8. MALIK J S, YENNURAJALINGAM S. Prokinetics and ghrelin for the management of cancer cachexia syndrome [J]. Ann Palliat Med, 2019, 8(1): 80-5.
9. LIM Y L, TEOH S E, YAOW C Y L, et al. A Systematic Review and Meta-Analysis of the Clinical Use of Megestrol Acetate for Cancer-Related Anorexia/Cachexia [J]. J Clin Med, 2022, 11(13).
10. ZHANG X, QIU H, LI C, et al. The positive role of traditional Chinese medicine as an adjunctive therapy for cancer [J]. Biosci Trends, 2021, 15(5): 283-98.
11. XU B, CHENG Q, SO W K W. Review of the Effects and Safety of Traditional Chinese Medicine in the Treatment of Cancer Cachexia [J]. Asia Pac J Oncol Nurs, 2021, 8(5): 471-86.
12. CHEN C, LV Q, LI Y, et al. The Anti-Tumor Effect and Underlying Apoptotic Mechanism of Ginsenoside Rk1 and Rg5 in Human Liver Cancer Cells [J]. Molecules, 2021, 26(13).
13. WANG Y S, ZHU H, LI H, et al. Ginsenoside compound K inhibits nuclear factor-kappa B by targeting Annexin A2 [J]. J Ginseng Res, 2019, 43(3): 452-9.
14. TO K I, ZHU Z X, WANG Y N, et al. Integrative network pharmacology and experimental verification to reveal the anti-inflammatory mechanism of ginsenoside Rh4 [J]. Front Pharmacol, 2022, 13: 953871.
15. YANG W, HUANG J, WU H, et al. Molecular mechanisms of cancer cachexia-induced muscle atrophy (Review) [J]. Mol Med Rep, 2020, 22(6): 4967-80.
16. ROM O, REZNICK A Z. The role of E3 ubiquitin-ligases MuRF-1 and MAFbx in loss of skeletal muscle mass [J]. Free Radic Biol Med, 2016, 98: 218-30.
17. YEOM E, YU K. Understanding the molecular basis of anorexia and tissue wasting in cancer cachexia [J]. Exp Mol Med, 2022, 54(4): 426-32.
18. MANTOVANI A, ALLAVENA P, SICA A, et al. Cancer-related inflammation [J]. Nature, 2008, 454(7203): 436-44.
19. FEARON K C, GLASS D J, GUTTRIDGE D C. Cancer cachexia: mediators, signaling, and metabolic pathways [J]. Cell Metab, 2012, 16(2): 153-66.
20. WEN W, SUN C, CHEN Z, et al. Alcohol Induces Zebrafish Skeletal Muscle Atrophy through HMGB1/TLR4/NF-kappaB Signaling [J]. Life (Basel), 2022, 12(8).
21. TANIGUCHI K, KARIN M. NF-kappaB, inflammation, immunity and cancer: coming of age [J]. Nat Rev Immunol, 2018, 18(5): 309-24.
22. BONETTO A, AYDOGDU T, JIN X, et al. JAK/STAT3 pathway inhibition blocks skeletal muscle wasting downstream of IL-6 and in experimental cancer cachexia [J]. Am J Physiol Endocrinol Metab, 2012, 303(3): E410-21.
23. ZHANG J, ZHENG J, CHEN H, et al. Curcumin Targeting NF-kappaB/Ubiquitin-Proteasome-System Axis Ameliorates Muscle Atrophy in Triple-Negative Breast Cancer Cachexia Mice [J]. Mediators Inflamm, 2022, 2022: 2567150.
24. ZHANG L, TANG H, KOU Y, et al. MG132-mediated inhibition of the ubiquitin-proteasome pathway ameliorates cancer cachexia [J]. J Cancer Res Clin Oncol, 2013, 139(7): 1105-15.
25. LEE S B, LEE J S, MOON S O, et al. A standardized herbal combination of Astragalus membranaceus and Paeonia japonica, protects against muscle atrophy in a C26 colon cancer cachexia mouse model [J]. J Ethnopharmacol, 2021, 267: 113470.
26. ACHARYYA S, GUTTRIDGE D C. Cancer cachexia signaling pathways continue to emerge yet much still points to the proteasome [J]. Clin Cancer Res, 2007, 13(5): 1356-61.
27. LAHA D, GRANT R, MISHRA P, et al. The Role of Tumor Necrosis Factor in Manipulating the Immunological Response of Tumor Microenvironment [J]. Front Immunol, 2021, 12: 656908.
28. WYKE S M, RUSSELL S T, TISDALE M J. Induction of proteasome expression in skeletal muscle is attenuated by inhibitors of NF-kappaB activation [J]. Br J Cancer, 2004, 91(9): 1742-50.
29. SGRIGNANI J, GAROFALO M, MATKOVIC M, et al. Structural Biology of STAT3 and Its Implications for Anticancer Therapies Development [J]. Int J Mol Sci, 2018, 19(6).
30. LU S, LI Y, SHEN Q, et al. Carnosol and its analogues attenuate muscle atrophy and fat lipolysis induced by cancer cachexia [J]. J Cachexia Sarcopenia Muscle, 2021, 12(3): 779-95.
31. CHEN L, CHEN L, WAN L, et al. Matrine improves skeletal muscle atrophy by inhibiting E3 ubiquitin ligases and activating the Akt/mTOR/FoxO3alpha signaling pathway in C2C12 myotubes and mice [J]. Oncol Rep, 2019, 42(2): 479-94.
32. RAUSCH V, SALA V, PENNA F, et al. Understanding the common mechanisms of heart and skeletal muscle wasting in cancer cachexia [J]. Oncogenesis, 2021, 10(1): 1.